Water, water everywhere and not a streamflow gauge in sight: Estimating freshwater inflows in an ungauged watershed at the Big Boggy National Wildlife Refuge, USA

Matthew J. Madewell (matthewmadewell20@gmail.com)
Texas A&M University https://orcid.org/0000-0003-0742-938X
Rusty A. Feagin
Texas A&M University
Thomas P. Huff
Texas A&M University
Bill Balboa
The Matagorda Bay Foundation

Research Article

Keywords: East Matagorda Bay, National Wildlife Refuge, freshwater inflows, bays and estuaries, coastal wetlands

Posted Date: June 23rd, 2022

DOI: https://doi.org/10.21203/rs.3.rs-1674114/v1

Abstract

Bays and estuaries often rely on freshwater inflows to maintain the salinity balance necessary to sustain their fisheries. Reduced freshwater inflows, particularly during summer seasons, can be detrimental to the health of these systems. Despite an extensive network of streamflow gauges in the U.S., many coastal watersheds remain ungauged. Our objective was to identify a way to quickly build a water budget for an ungauged watershed, using limited data, to determine its freshwater inflow contributions to an estuary. We developed and tested this method for Big Boggy Creek, which flows into East Matagorda Bay (EMB), Texas. Streamflow into and out of Big Boggy Creek was quantified at key upstream and downstream points. Over the study period, we found average monthly freshwater inflows of 1,897 megaliters (ML). Historic and predicted freshwater inflows over a longer time period were calculated using a data-driven model, based on our water budget. Historic monthly inflows for this model averaged 2,000 ML from 1953 to 2019 for Big Boggy Creek. Predicted inflows followed three climate scenarios outlined by the Intergovernmental Panel on Climate Change. Using these findings, we developed an inflow decision tool to assist resource managers in assessing future freshwater inflows into EMB. We show two inflow improvement actions for EMB that can be informed by using this tool—purchasing water from the local river authority and increasing the effective watershed. The approaches developed in this study can be applied to similarly ungauged watersheds to budget, model, and predict their freshwater inflow contributions to estuaries.

Introduction

Bays, estuaries, and coastal wetlands depend on an adequate supply of freshwater from inland rivers (Montagna et al. 2002). Freshwater inflows are critical to the survival of estuarine organisms through two main avenues: maintaining the salinity gradient and providing sediments and nutrients to the system (Palmer, Montagna, and Kalke 2002). For example, bays along the Texas coast span the salinity gradient, from Galveston Bay on the Upper Texas Coast containing salinities of 1.8 to 28 Practical Salinity Units (PSU) to the Laguna Madre on the South Texas Coast with salinities equal to or greater than 35 PSU (National Oceanic and Atmospheric Administration 2022). Each respective bay system and its aquatic inhabitants have adapted to its freshwater inflow regime and salinity gradient. For example, while oyster reefs are uncommon in the hypersaline Laguna Madre, what oysters are present have adapted to the hypersaline conditions and may not survive at lower levels of salinity (Marshall 2021). Conversely, if inflows become limited in bays with typically low salinity, we may expect to see salinities reach levels too high for local flora and fauna to tolerate. An adequate freshwater inflow regime helps maintain ecological resilience in bays, estuaries, and coastal wetlands.

Sediment and nutrient influxes are another crucial aspect of freshwater inflows. Sediments delivered by inland rivers help maintain mudflat and salt marsh accretion (Bouma et al. 2016; Wang, Lu, and Sikora 1993). Without these sediment inputs, salt marsh accretion can be stymied and the ability of salt marshes to withstand relative sea level rise (RSLR) can be threatened. Widespread loss of salt marsh is a threat to the health of bays and estuaries due to the large number of benthic and pelagic organisms that use salt marshes at some point in their life cycle (Rozas and Minello 1998). Nutrients are also supplied by freshwater inflows, which support the higher levels of the trophic pyramid. Nutrient inputs can also arrive via freshwater inflows, and these can have positive or negative effects, such as supporting primary production through plankton and benthic organism, or instigating algal blooms and eutrophication (Howarth 1988; Turner and Rabalais 1994; Valiela et al. 1992).

It is thus important to quantify the volume of freshwater inflows to bays, estuaries, and coastal wetlands. As of 2018, 8,580 river gauges across the US measured both streamflow and water level, and an additional 1,750 only measured water level (Eberts et al. 2019). The distribution of these streamflow gauges includes most major rivers, yet leaves thousands of smaller watersheds ungauged. While flows for ungauged inland streams may ultimately be captured by streamflow gauges further downstream on the mainstem of a river, coastal watersheds flow directly into bays, estuaries, or the ocean. Therefore, the flows from a large majority of ungauged coastal watersheds are never quantified, and without this knowledge coastal managers cannot establish environmental flow standards for their downstream bays, estuaries, and coastal wetlands.

East Matagorda Bay (EMB) in Texas provides an excellent example of the types of problems that ungauged watersheds can present for coastal managers. For this estuary, the Colorado River of Texas no longer provides direct freshwater inflows to EMB, after extensive human modification re-routed its flows (Clay 1949). Today, the only freshwater inflows to EMB are attributed to a few small ungauged watersheds, such as that of Big Boggy Creek. These watersheds may not be providing adequate freshwater inflows to EMB, fostering concern that EMB will become increasingly hypersaline and negatively impact commercial and recreational fisheries. Freshwater inflows into EMB have been modeled since 2003 when the Texas Water Development Board (TWDB) began studying EMB (Schoenbaechler, Guthrie, and Lu 2011). However, the models were based on rainfall-runoff estimates from the Texas Rainfall-Runoff (TxRR) model which does not use empirical inflow data—due to a lack of gauged rivers in the watersheds that drain into EMB. We thus sought to bridge the gap between modeled and actual freshwater inflows contributing to EMB.

Our overall objective was to develop a data-driven approach that could predict freshwater inflows over relatively long time periods, when given a limited quantity of streamflow measurements for a relatively small and ungauged watershed. We sought to develop this approach for Big Boggy Creek in EMB, and then build a tool that could aid resource managers and policymakers to set environmental standards for its flows. Specifically, we sought to (1) quantify average streamflow rates into and out of this watershed to build a water budget; (2) construct a data-driven model to estimate its historic and future inflows; and (3) identify restoration actions to increase its inflows into EMB. Finally, we discuss how this approach can be applied to other ungauged coastal watersheds.

Methods

Study area

Big Boggy Creek is a coastal watershed that drains into East Matagorda Bay (EMB) eight miles northeast of Matagorda, Texas, USA (Fig. 1). The southern Big Boggy Creek watershed consists of alluvium deposits created during the Holocene, deposited by Big Boggy Creek and Peyton Creek watersheds (Texas Water Science Center 2014). The southern reaches of the watershed are dominated by salt marshes. The northern Big Boggy Creek watershed lies on the Beaumont Formation from the Late Pleistocene. In the northern reaches of the watershed, Big Boggy Creek flows through cattle pastures with stream banks maintained and mowed periodically by the Matagorda County Drainage District. Several weir structures are present along Big Boggy Creek that impede aquatic movement upstream and may limit freshwater flow downstream.

Hydrologically, the study area consists of Big Boggy Creek which flows along the western side of the study area. A handful of small unnamed tributaries flow into Big Boggy Creek along its longitudinal gradient. There are also several irrigation canals or ditches that appear to connect to Big Boggy Creek near its headwaters northwest of Wadsworth, Texas. Historically, there had been one U.S. Geological Survey (USGS) streamflow gauge deployed on Big Boggy Creek near Wadsworth, Texas from 1970 to 1977. This gauge was located at the northern extent of the study area and as such, does not include the large majority of inflow sources that connect much further downstream, nor the large majority of the volume that eventually reaches EMB. At approximately six stream kilometers from its mouth, Big Boggy Creek transitions from its narrow channel to a wider form dominated by *Spartina alterniflora* in an expansive salt marsh complex that occupies an area of almost 900 hectares. This salt marsh complex extends six kilometers eastward from Big Boggy Creek to Chinquapin Road (this road lies at the location of the easternmost star in Fig. 1). Chinquapin Road serves as a line of demarcation between the Big Boggy Creek and Lake Austin watersheds. However, an unobstructed culvert beneath Chinquapin Road hydrologically connects the two watersheds. The Gulf Intracoastal Waterway (GIWW) forms the southern edge of the study area and separates Big Boggy Creek from EMB.

The study area encompasses the entire Big Boggy Creek watershed (Fig. 1), which includes 1,500 acres of the Big Boggy National Wildlife Refuge (NWR) under operation by the U.S. Fish & Wildlife Service (FWS). The remaining portion of the study area is privately owned and functions primarily as cattle grazing pasture. Ninety acres of rice paddies are present at Big Boggy NWR, all of which are seasonally planted with ryegrass to provide winter browse for waterfowl (FWS 2013).

Quantify average streamflow rates into and out of the watershed to build a water budget

The characteristics of the hydrological network were quantified using a series of sensors and gauges that were placed in the field. A model of the water budget for the watershed was then developed that incorporated the watershed area, precipitation, and integrated the field data. The resulting model helped determine the supplemental inflows required monthly to maintain inflows within a suitable historical range and forecast the future needs of the system under changing precipitation regimes.

Sensors

Sensors were deployed from June 23, 2020, through March 5, 2021 (see Table 1 for detailed deployment dates). The sensors included Conductivity, Temperature, and Depth (CTD) dataloggers (CTD-Diver, Van Essen Instruments), Solinst Leveloggers (Levelogger 5 LTC, Solinst Canada Ltd.), Acoustic Doppler Current Profilers (ADCP; Aquadopp Profiler 1 MHz, Nortek Group), and a precipitation gauge (Onset tipping bucket rain gauge). The CTD dataloggers contained a pressure sensor that measured the hydrostatic pressure of the water to calculate total water depth, as well as a 4-electrode conductivity sensor that measured the specific conductivity of the water—a proxy for salinity. CTD dataloggers were set to record hourly measurements and deployed in a PVC pipe securely inserted into the stream bottom. The ADCP units use acoustic Doppler sensors to measure the flow speed of the water column. The ADCP units were affixed to a steel frame, anchored to a fence post using coated steel cables, and placed at the center of the stream channel. The precipitation gauge was deployed near the other sensors and recorded the amount of rainfall occurring for each rainfall event. Additional hourly precipitation data was obtained from the Lower Colorado River Authority (LCRA) rain gauge at Matagorda, Texas (Gauge Matagorda 1 S), 10 miles southwest of the study area.

Table 1
Sensor deployment locations and dates

Equipment Deployment Dates			
Sensor Group	**Sensor Type**	**Start**	**End**
1 - North Boggy	ADCP	6/23/2020	9/19/2020
1 - North Boggy	CTD	6/23/2020	3/5/2021
1 - North Boggy	ADCP	4/9/2021	6/15/2021
1 - North Boggy	CTD	4/9/2021	6/15/2021
1 - North Boggy	HOBO rain gauge	4/9/2021	6/15/2021
2 - South Boggy	ADCP	7/3/2020	9/19/2020
2 - South Boggy	CTD	7/3/2020	3/5/2021
2 - Upland	Barometer	6/23/2020	3/5/2021
3 - Pelton Lake	Solinst	6/23/2020	3/5/2021
3 - Pelton Lake	HOBO rain gauge	6/23/2020	9/19/2020
3 - Chinquapin	CTD	7/3/2020	3/5/2021

The sensors were deployed at three stations (Fig. 1). The “Upper Boggy” station (UB) contained an ADCP and CTD sensor and was placed upstream of the salt marsh complex and north of Big Boggy NWR, where the creek banks were more riverine in form and the vegetation indicative of brackish conditions. This station primarily measured the freshwater inflow entering the refuge by way of Big Boggy Creek. The “Lower Boggy” station (LB) was placed further south within the salt marshes of Big Boggy NWR, near the mouth of Big Boggy Creek where it intercepts the Gulf Intracoastal Waterway (GIWW). This second station also had an ADCP and CTD but primarily measured tidal flow in and out of the watershed. A third group of sensors consisting of a Solinst Levelogger and precipitation gauge was placed along the eastern edge of Pelton Lake, and an additional CTD gauge was placed in Chinquapin Bayou on the east side of Chinquapin Road, on the other side of a culvert. This group of sensors was put in place to identify the degree of hydrologic isolation of Pelton Lake and its connectivity with Chinquapin Bayou. Unfortunately, the Solinst sensor deployed in Pelton Lake suffered a critical failure that rendered the data unrecoverable. The relationship between the Big Boggy Creek and Lake Austin watersheds were thus identified using only the CTD at Chinquapin Road.

The water level data from the CTD sensors and the flow rate data from the ADCP sensors were then vertically referenced into North American Vertical Datum (NAVD88) units, using a survey-grade Global Navigation Satellite System (GNSS). We then cross-referenced our datasets with the National Oceanic and Atmospheric Administration’s (NOAA) Matagorda City tidal gauge (Station ID: 8773146) nine kilometers southwest of the study area.

Hourly stream flow volumes were calculated by multiplying the ADCP-measured, depth-averaged water velocities in each direction by the cross-sectional area of the channel. The cross-sectional area also varied each hour based on the water level height, and this height was identified by using the accompanying CTD datasets (channel width * hourly water level depth = hourly cross-sectional area). Upstream and downstream flows were determined using the ADCP directional measurements.

Water Budget

A water budget was developed using the sensor datasets to determine the amount of monthly freshwater inflows to EMB. To better parse out the inflow contributions, the water budget was divided into two sub-watersheds based on the UB and LB stations. At each location, we accounted for the differences between the upstream-versus-downstream flow volumes and then related them to the precipitation and effective watershed size. Groundwater was not explicitly accounted for in this water budget (see Discussion).

The water budget variables at each station included downstream flows, upstream flows, and precipitation. Although we had hourly data available for each of these variables over longer time frames at various stations, we chose to only use data from 7/4/2020 to 9/19/2020 to build the budget for dates in which both ADCP stations were active. During this period, the precipitation balance was just below the mean for the period over the past several decades (see Results for more).

This July-August-September period (hereby referred to as “summer”) was uniquely important because it is during these summer months when temperatures are highest and hypersalinity or hypoxia can occur. The water budget variables were aggregated over the entire three-month period based on an initial investigation of the relationship between precipitation and flow, wherein we concluded that these three months of data were not sufficiently long enough for us to quantitatively account for timing delays caused by complex watershed effects and antecedent conditions. Similarly, there may be limitations in the dataset due to the relatively short period of record. It is possible that flows during our summer period of record do not reflect flow patterns for other periods throughout the year, yet this is the challenge that we set – to develop a methodology to identify inflows for previously ungauged watersheds with limited data availability.

For each station, the imbalance between upstream and downstream flow volume was found. Upstream flows could include both incoming tides and storm surges. Downstream flows could include outgoing tides and freshwater flows from upstream reaches of the watershed. Then, the precipitation volume was calculated for the sub-watersheds that fed into each station. To do this, we obtained the precipitation from the Water Data for Texas website operated by the Texas Water Development Board (TWDB) (Texas Water Development Board 2021). This precipitation dataset combines data from different precipitation stations within a quadrant to estimate precipitation throughout the entire quadrant. These datasets were then multiplied by the "total watershed area" and the "effective watershed area" for each station. The total watershed area was identified using the Watershed tool in ArcGIS Pro and a 1-meter Digital Elevation Model (DEM); two "total watershed" products were produced to delineate the separate sections of the landscape that uniquely contributed to the UB and LB stations. The effective watershed area was defined as the area across which the precipitation could be assumed to have fallen (minus any evaporation), that would then be equivalent to the observed quantity of inflow reaching each station. In other words, the effective watershed area is the area of capture that is multiplied by a precipitation measurement to obtain the amount of precipitation-driven inflows (upstream minus downstream flows) that are observed flowing past our sensor station.

Estimate historic and future inflows

The water budget model was used to hindcast and forecast the freshwater inflow volume at the Upper Boggy and Lower Boggy stations from 1954 to 2100. Because of the relatively short period of data collection (6/23/2020-3/5/2021 for CTDs; 7/4/2020-9/19/2020 for ADCPs), there was additional uncertainty in hindcasting and forecasting, due to the potential variability in how the watershed reacts to periods of high or low precipitation. Because of this, the forecasting scenarios were estimated based on the mean trend. The estimated historic freshwater inflows for each year from 1954 to 2019 were aggregated during the same summer months as the budget. The values were derived from the TWDB precipitation dataset, in the same manner as for the budgeting described previously.

The mean trend across the historical period and the root-mean-square error (RMSE) were calculated to identify past years where net flows were above and below what was considered a typical summer for rainfall in the region. The mean trend line and the RMSE ranges were graphed to help depict the most aberrant years. For the aberrant years that fell outside of and below the lower RMSE bound (the drought years), we calculated the amount of supplementary inflow that would be needed to bring the total inflow back up to the lower RMSE bound, as well as back up to the mean. These two values make up the estimated range of supplemental volume that would be needed to bring the inflow out of low flow conditions.

Three climate change scenarios were used to forecast changes in freshwater inflows during the same budgeted months. The three climate change scenarios were defined by the Intergovernmental Panel on Climate Change (IPCC) and statistically downscaled to be region-specific by Jiang and Yang (2012), and include the A1B, A2, and B1 scenarios. Each scenario predicts future trajectories of climate change depending on global changes in demographics, and economical or technological developments (Nakicenovic et al. 2000), wherein A2 is the most negatively severe outcome, A1B is intermediate, and B2 is the most favorable.

Results

Quantify average water flow rates into/out of the watershed and create a water budget

Water level and salinity at all three stations were affected by both tides and precipitation events (Fig. 2). During the entire record, four tropical events passed by the area. However, during the more limited period of the water budget (7/4/2020–9/19/2020), only two tropical cyclones passed by the area, Hurricane Hanna and Hurricane Laura, and the precipitation observed during this period was 24 cm (9.5 in.) Precipitation throughout 2020 (32.36 cm) was 5% lower than the average rainfall from 1954 to 2020 (34.12 cm).

The UB station was most responsive to precipitation as shown with its brief peaks following precipitation events, followed by a generally rapid return to its baseline. At the LB station, water level is largely driven by the tides and storm surges. Precipitation can also cause water levels at LB to rise, just slightly below those at UB (1.4 m at UB compared to 1.3 m at LB on September 22, 2020). The Chinquapin Road station was the most unique of the three. At times, the Chinquapin Road station appeared to respond differently to precipitation events, and the water levels generally took longer to decrease after these events, suggesting that it was responding to different inflow sources (i.e., Lake Austin). Further, the daily tidal range at Chinquapin Road was 4 cm, the lowest of the three stations, potentially indicating a hydrologically isolated location.

The ADCPs provided stream flow volume and direction (Fig. 3). When coupled with water elevation data from the accompanying CTD, we obtained a more complete understanding of flows at the UB and LB stations. The volume of flow between UB and LB can differ drastically. At the peak of Hurricane Hanna (July 25, 2020), almost 65,000 m^3/hour was flowing at LB. In contrast, the peak upstream flow at UB was only 19,000 m^3/hour. The flow volumes also varied drastically during regular tidal periods, with a difference of almost 5,000 m^3/hour between the incoming and outgoing tides and at LB, and a difference of only 200 m^3/hour at UB. As shown in Fig. 3b, the downstream flows at LB were not in balance with upstream flows. This supports the notion that there were alternate outlets for LB flow exiting into the GIWW (other than Big Boggy Creek).

Hydrological Budget

At the UB station, the total upstream flow during the budgeted period of 7/4/2020 to 9/19/2020 was 1,390 ML (Fig. 4) consisting of incoming tides. Total downstream flow measured 2,120 ML, consisting of outgoing tides and freshwater flows. The imbalance between upstream and downstream flows was 730 ML and represented the freshwater inflow quantity. It thus represented the difference between the total precipitation and evaporation in the watershed further upstream, excepting any unbudgeted losses or gains (see Methods).

The total watershed area upstream of the UB station was 7,927 hectares. The quantity of precipitation multiplied by this area resulted in a far higher value than the 730 ML observed inflow volume. Thus, the effective watershed area was calculated as 225 hectares, which was only 2.84% of the total watershed area (Fig. 5). This quantity matched what could be expected given direct capture of precipitation into the system. In other words, our sensor stations may have only observed precipitation that fell into open water bodies, low marsh, and high marsh areas, insinuating that overland flows did not play as large a role as previously assumed. Low topographical relief in the study area may explain this phenomenon. Flat upland areas may not readily flow into the waterways and instead be subject to high rates of evaporation.

At the LB station, the total upstream flow during the study period was 6,652 ML, consisting of incoming tides and storm surges. Total downstream flow measured 4,220 ML, consisting of outgoing tides and freshwater flows. The difference between upstream and downstream flows was 2,431 ML. Precipitation was estimated as 4,961 ML.

We found that the total watershed area upstream of the LB station—and downstream of UB—was 2,780 hectares (Fig. 5). The effective watershed area was calculated as 1,532 hectares, which was 55% percent of the total potential area. This percent was much higher compared to UB, because much of the LB watershed was effectively directly capturing the precipitation in open water, low marsh, or high marsh areas.

It is important to note that there was a large imbalance in the water budget at LB. There was approximately 7,392 ML unaccounted for as calculated by the effective watershed. This imbalance value includes upstream flows as well as precipitation. When taking into consideration the downstream flows from UB into LB (2,120 ML), there was a total of 9,502 ML. This large surplus of water suggests that there were other significant outlets in the marsh complex (Fig. 6). These outlets likely only connect and move water out of the marsh complex and into the GIWW when water levels exceeded 0.45 m (NAVD88). The only alternate outlet that may not be water-level dependent was the culvert beneath Chinquapin Road. Groundwater flux may account for some of this loss, however it likely does not account for much of the volume as we would generally not expect tidal waters to flow into groundwater in this coastal area due to hydraulic head pressure.

Hindcasted and forecasted inflow volumes

We found that the average historic inflows at UB and LB were 255 Megaliters (ML) per month and 1,744 ML per month (in July, August, and September), respectively. Hindcasted inflows followed a positive mean trend, increasing over this budgeted time period from 1954 to 2019 (Fig. 7). Note that for each historic year only the three summer months were used to match the study period. Over the historic period, nine years were above the positive RMSE threshold and seven years were below the negative RMSE threshold. Of the three climate change scenarios through 2100 that were explored, the best-case scenario was the B1 scenario, in which a 4% increase in inflow was predicted. The intermediate scenario, A1B, estimated a 3% increase in inflow. Finally, A2 yielded the worst-case prediction, where inflows were predicted to decrease by 4%. It is crucial to note that these were just predicted changes in the mean trend of inflow. Years with inflows higher or lower than the mean and outside of the RMSE bounds will occur, and these are more likely to alter ecosystem function than a change in the mean trend.

Discussion

There are two key outcomes to this research. First, we present a simple framework for estimating freshwater inflows that can be replicated in other tidally influenced watersheds. Ungauged watersheds far outnumber gauged watersheds in coastal zones across the globe. While region-specific variables need to be accounted for, researchers in virtually any coastal setting can use our study as a framework to determine freshwater inflows in ungauged watersheds.

Second, we have estimated the freshwater inflow contribution of the Big Boggy Creek watershed to East Matagorda Bay (EMB). Hindcasted values suggest that the mean trend in freshwater inflows has been increasing since 1954. Forecasted values suggest that this trend is also likely to increase, or at least change by a magnitude quite small relative to the year-to-year variation that can occur. These findings have important implications for setting environmental flow standards for EMB—rather than inflows being the issue, their circulation or consistent delivery throughout the estuary may be the biggest issue facing EMB in the future.

The natural processes which sustained EMB and the surrounding salt marshes prior to the re-routing of the Colorado River have left EMB without its former source of freshwater and sediment (Buzan et al 2011). Resource managers and policymakers cannot turn back the clock to pre-Colorado River conditions, they can however instead focus on delivering consistent freshwater inflows when EMB needs it most—during summer periods of low flows and high temperatures.

For this reason, we developed a decision tool to better synthesize our resulting model and put it into the hands of resource managers and stakeholders (the tool is available at cml.tamu.edu). The excel-based tool requires a user to input monthly precipitation data from the TWDB Water Data for Texas website or the LCRA precipitation gauge located in Matagorda, Texas. This input is next multiplied by the effective watershed area to find the estimated total precipitation-driven freshwater inflows. This volume is then compared to the mean trend and the upper and lower bounds as determined by the mean ± RMSE. The tool then calculates the volume of supplementary water that would need to be added to Big Boggy Creek in order to meet the upper and lower bounds. Finally, the tool converts this volume into the surface area of additional effective watershed that would be needed to capture this volume.

Potential management and restoration actions to increase inflow

As part of its duties, the LCRA sells water to users in the Lower Colorado River basin for municipal, agricultural, and wildlife management uses (Austin et al. 2015). Existing agriculture in the area utilizes irrigation canals to transport water, and at least one of the canals is adjacent to the center portion of the NWR (FWS 2013). In 2021, water purchases from LCRA were available at a rate of $81.55 per ML delivered ($66.14 per acre-foot; E. Ray, personal communication, October 26, 2021). If the historic 2011 drought happened in the summer of 2021, it would cost ~$14,000 per month to return the conditions to within the normal RMSE bounds. To put this cost into perspective, the ex-vessel value for commercial fisheries landings in EMB was $317,458 in 2019 alone (Texas Parks and Wildlife Department 2015). The cost of purchasing freshwater is therefore relatively low compared to the economic value of fisheries in EMB.

An alternative perspective is to think about how much land is needed to capture precipitation and convert it into supplemental inflow—in other words, to increase the effective watershed area and rely on precipitation rather than purchasing supplemental flows. Resource managers can use the inflow decision tool to estimate the additional effective watershed area needed to offset the decline in inflows. Using the 2011 drought as an example, an additional 362 hectares would be needed to meet the lower bound, and 885 hectares would be needed to reach the mean trend. A series of impounded ponds located immediately north of Big Boggy NWR present themselves as potential restoration targets, but the effective watershed area would increase by only 17 hectares. An additional 386 hectares of upland areas could also be graded to drain into an existing channel more readily and facilitate upslope marsh migration in response to sea level rise. However, most of these lands are privately owned and incentives would likely be necessary for landowner cooperation (e.g., fee simple land acquisition or conservation easements). In summary, the most realistic and immediately impactful action would be to purchase water through the LCRA during times of drought.

Limitations and directions for further study

As stated previously, the framework presented here can be applied to other ungauged coastal watersheds. Without making any significant changes to the methodology, researchers can similarly develop a water budget with only a few months of field data. However, we have identified three modifications that could be made to improve results.

Groundwater flux is notoriously difficult to quantify in aquatic settings, requiring specialized equipment and complicated methods. This was a limitation to our study, although groundwater is likely less relevant in EMB as compared to other potential locations. Previous studies on Beaumont Formation sediments suggest that there is low vertical hydraulic conductivity but a relatively high horizontal hydraulic conductivity in these formations (Capuano and Jan 1996; Soil Survey Staff 2021). This indicates that there is likely to be exchange between surface water and groundwater, however, a lack of region-specific data hinders our ability to estimate the net porewater exchange. In a review of salt marsh hydrogeology, Guimond and Tamborski (2021) found a positive relationship between tidal range and submarine groundwater discharge. Due to the low vertical hydraulic conductivity and microtidal regime—and hence low submarine groundwater discharge—it is assumed that the exchange of surface water and groundwater balances out over the study period. The high horizontal hydraulic connectivity paired with the low vertical hydraulic conductivity creates an environment where there is water exchange between surface water and the marsh platform, but not significant vertical movement of water. Future studies should consider implementing seepage meters (Rosenberry 2008) or mini-piezometers (Martinez 2010) to quantify surface water—groundwater exchange. This should be replicated at as many transects in the study area as feasible and at different times of year as hydrological data is collected.

Plant evapotranspiration (ET) is another potential component to include in a water budget. While outside the scope of this study, ET from both wetland and terrestrial plants could provide an additional pathway for water export from the Big Boggy Creek watershed. Quantifying the loss via ET could be accomplished using various methods. Lysimeters reveal plants water use by continuously weighing a block of soil (Sturtevant 1919; Rana and Katerji 2000). This method is intrusive and difficult, requiring excavation and installation of a lysimeter. Alternately, one could measure vapor flux with an eddy covariance (EC) tower. EC towers use micrometeorological techniques to measure various exchanges, including water, between the biosphere and the atmosphere (Baldocchi, Hicks, and Meyers 1988). These towers can be expensive (Billesach et al. 2004; Markwitz and Siebicke 2019) ranging in cost from $16,000 to $25,000. The inclusion of ET no doubt increases the complexity of creating a water budget, and it may be most important in locations where the water is already impounded and thus not a part of the effective watershed area.

As with nearly all studies, more data—in this case a longer time series—would lend itself to a more accurate budget and model. For most ungauged watersheds, however, there are constraints due to geographical isolation, limited financial resources, and unforeseen events. For example, we withdrew our ADCP sensors from the field after only three months due to the threat posed by Tropical Storm Beta. This time period had two hurricanes and several thunderstorms and should provide a good sample of the potential range of freshwater inflows in our study area from July to September. However, it is certainly possible that the Big Boggy Creek watershed behaves differently under different antecedent conditions. For example, surface water infiltration and overland flow rates may be different under pre-existing drought conditions, even if the exact same quantities of precipitation occurred. Studies conducted in forest (Gimbel, Puhlmann, and Weiler 2015) and blanket peatland (Holden and Burt 2002) settings have demonstrated this phenomenon. There may be unidentified watershed-specific features that do not provide freshwater inflows until a certain precipitation volume or intensity threshold is surpassed. A larger dataset that encompasses different seasons and various extremes is the simplest way to address these concerns. However, a lack of data was the key driver behind this study in the first place and tends to be a ubiquitous issue for small watersheds. Even when extreme weather, a lack of funding, faltering equipment, or geographical isolation come into play, one may still need to develop a water budget for management purposes.

Conclusion

This study provides a simple framework that can be replicated in other ungauged watersheds to quantify freshwater inflows to bays, estuaries, and coastal wetlands. As shown in the example of Big Boggy Creek and EMB, freshwater inflows can be quantified with field data, and then related to longer time period data through modeling. Managers can then use such findings to help purchase supplemental water during periods of drought and thus ensure estuarine and coastal wetland sustainability.

Declarations

Funding

This work was made possible by the Texas Water Development Board under Grant Number 2000012414. Its contents are solely the responsibility of the authors and do not necessarily represent the official views of the Texas Water Development Board.

Competing Interests

The authors have no relevant financial or non-financial interests to disclose.

Data Availability

The datasets generated during the current study are available at cml.tamu.edu.

Author contributions

MJM, RAF, TPH designed the research; MJM, TPH, BB performed the data collection duties, assisted in field efforts, MJM, TPH analyzed data. MJM, RAF primarily wrote the manuscript, and all have edited it.

References

1. Austin B, Kennedy A, Osting T, Walker C (2015) Evaluation of Freshwater Delivery Alternatives to East Matagorda Bay. AquaStrategies.
2. Billesbach DP, Fischer ML, Torn MS, Berry JA (2004) A Portable Eddy Covariance System for the Measurement of Ecosystem–Atmosphere Exchange of CO2, Water Vapor, and Energy. Journal of atmospheric and oceanic technology 21:639-650. doi: 10.1175/1520-0426(2004)021<0639:APECSF>2.0.CO;2.

3. Bouma TJ, van Belzen J, Balke T, van Dalen J, Klaassen P, Hartog AM, Callaghan DP, Hu Z, Stive MJF, Temmerman S, Herman PMJ (2016) Short-term mudflat dynamics drive long-term cyclic salt marsh dynamics. Limnology and oceanography 61:2261-2275. doi: 10.1002/lno.10374.
4. Buzan D, Cook B, Fontenot M, Hardy T, Hoffpauir R, Kennedy K, Thornton O, Trungale J, Wakefield C, Watters S (2011) BBEST Environmental Flow Regime Recommendations Report. Colorado and Lavaca Rivers and Matagorda and Lavaca Bays Basin and Bay Expert Science Team.
5. Capuano RM, Jan RZ (1996) In Situ Hydraulic Conductivity of Clay and Silty-Clay Fluvial-Deltaic Sediments, Texas Gulf Coast. Ground water 34:545-551. doi: 10.1111/j.1745-6584.1996.tb02036.x.
6. Clay C (1949) The Colorado River Raft. Southwestern historical quarterly 52:410-426.
7. Eberts SM, Woodside MD, Landers MN, Wagner CR (2019) Monitoring the pulse of our Nation's rivers and streams—The U.S. Geological Survey streamgaging network. Fact Sheet.
8. Gimbel KF, Puhlmann H, Weiler M (2015) Does drought alter hydrological functions in forest soils? An infiltration experiment. Hydrology and earth system sciences discussions 12:7689-7725. doi: 10.5194/hessd-12-7689-2015.
9. Guimond J, Tamborski J (2021) Salt Marsh Hydrogeology: A Review. Water (Basel) 13:543. doi: 10.3390/w13040543.
10. Holden J, Burt TP (2002) Laboratory experiments on drought and runoff in blanket peat. European journal of soil science 53:675-690. doi: 10.1046/j.1365-2389.2002.00486.x.
11. Howarth R (1988) Nutrient limitation of net primary production in marine ecosystems. Annual review of ecology and systematics 19:89-110. doi: 10.1146/annurev.ecolsys.19.1.89.
12. Jiang X, Yang Z (2012) Projected changes of temperature and precipitation in Texas from downscaled global climate models. Climate research 53:229-244. doi: 10.3354/cr01093.
13. Markwitz C, Siebicke L (2019) Low-cost eddy covariance: a case study of evapotranspiration over agroforestry in Germany. Atmospheric measurement techniques 12:4677-4696. doi: 10.5194/amt-12-4677-2019.
14. Marshall DA, Casas SM, Walton WC, Rikard FS, Palmer TA, Breaux N, La Peyre MK, Beseres Pollack J, Kelly M, La Peyre JF (2021) Divergence in salinity tolerance of northern Gulf of Mexico eastern oysters under field and laboratory exposure. Conservation physiology 9:coab065. doi: 10.1093/conphys/coab065.
15. Martinez C (2010) Mini-piezometers for Measuring Groundwater to Surface Water Exchange. EDIS 2010.
16. Montagna P, Alber M, Doering P, Connor M (2002) Freshwater Inflow: Science, Policy, Management. Estuaries 25:1243-1245. doi: 10.1007/BF02692221.
17. Nakicenovic N, Alcamo J, Davis G, de Vries B, Fenhann J, Gaffin S, Gregory K, Grubler A, Jung TY, Kram T, La Rovere EL, Michaelis L, Mori S, Morita T, Pepper W, Pitcher HM, Price L, Riahi K, Roehrl A, Rogner H, Sankovski A, Schlesinger M, Shukla P, Smith SJ, Swart R, van Rooijen S, Victor N, Dadi Z (2000) Special Report on Emissions Scenarios : a special report of Working Group III of the

Intergovernmental Panel on Climate Change. Cambridge University Press, New York, NY (US), United States.

18. Palmer T, Montagna P, Kalke R (2002) Downstream Effects of Restored Freshwater Inflow to Rincon Bayou, Nueces Delta, Texas, USA. Estuaries 25:1448-1456. doi: 10.1007/BF02692238.
19. Rana G, Katerji N (2000) Measurement and estimation of actual evapotranspiration in the field under Mediterranean climate: a review. European Journal of Agronomy 13:125-153.
20. Rosenberry DO (2008) A seepage meter designed for use in flowing water. Journal of hydrology (Amsterdam) 359:118-130. doi: 10.1016/j.jhydrol.2008.06.029.
21. Rozas L, Minello T (1998) Nekton Use of Salt Marsh, Seagrass, and Nonvegetated Habitats in a South Texas (USA) Estuary. Bulletin of marine science 63:481-501.
22. Schoenbaechler C, Guthrie C, Lu Q (2011) Coastal Hydrology for East Matagorda Bay. Texas Water Development Board.
23. Soil Survey Staff, Natural Resources Conservation Service, United States Department of Agriculture. (2021) Web Soil Survey. Available online at the following link: http://websoilsurvey.sc.egov.usda.gov/. Accessed 5 May 2021
24. Sturtevant EL (1919) Sturtevant's notes on edible plants. J.B. Lyon Co., State Printers, 1919, New York (State).
25. Texas Parks and Wildlife Department (2015) Trends in Texas Commercial Fishery Landings, 1994-2012.
26. Texas Water Development Board (2021) Lake Evaporation and Precipitation. Water Data for Texas. https://www.waterdatafortexas.org/lake-evaporation-rainfall. Accessed 10 June 2021
27. Turner RE, Rabalais NN (1994) Coastal eutrophication near the Mississippi river delta. Nature (London) 368:619-621. doi: 10.1038/368619a0.
28. United States Department of Agriculture. (1953). Matagorda USDA historic imagery, 1953-02-08.
29. United States Department of Agriculture. (2020). Texas NAIP imagery, 2020-04-01.
30. United States Fish and Wildlife Service (2013) Texas Mid-Coast National Wildlife Refuge Complex, Brazoria, Fort Bend, Matagorda, and Wharton Counties, TX; Comprehensive Conservation Plan and Environmental Assessment. Interior Department Documents and Publications.
31. United States Geological Survey (2016) USGS Water Data for the Nation.
32. Valiela I, Foreman K, LaMontagne M, Hersh D, Costa J, Peckol P, DeMeo-Andreson B, D'Avanzo C, Babione M, Sham CH, Brawley J, Lajtha K (1992) Couplings of Watersheds and Coastal Waters: Sources and Consequences of Nutrient Enrichment in Waquoit Bay, Massachusetts. Estuaries ESTUDO, Vol. 15, No. 4, p 443-457, December 1992. 14 fig, 5 tab, 22 ref.
33. Wang FC, Lu T, Sikora WB (1993) Intertidal Marsh Suspended Sediment Transport Processes, Terrebonne Bay, Louisiana, U.S.A. Journal of Coastal Research JCRSEK, Vol. 9, No. 1, p 209- 220, Winter 1993. 7 fig, 4 tab, 33 ref. USGS Contract No. 14-08-0001-23413.

Figures

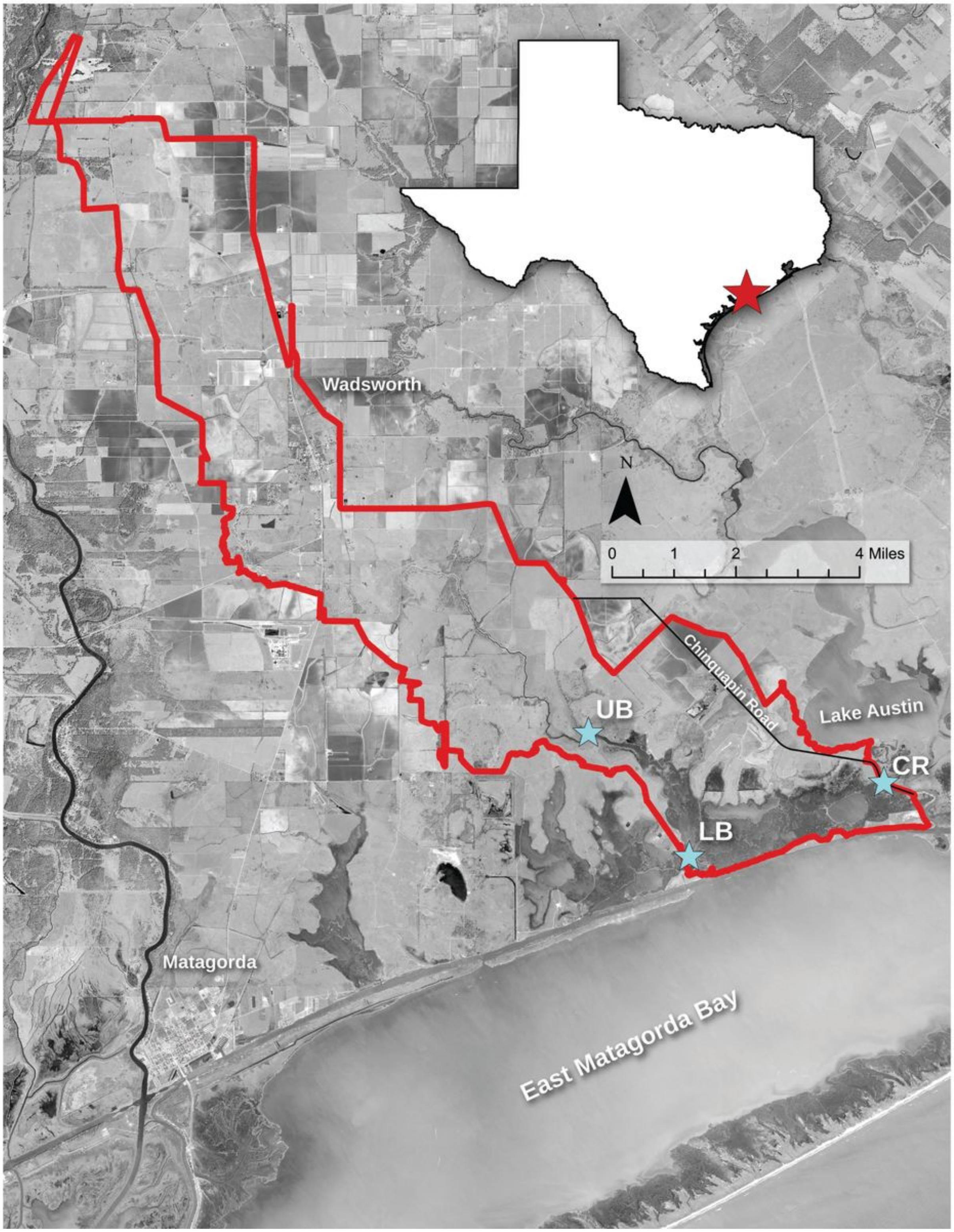

Figure 1

Project study area located 70 miles southwest of Houston, Texas. The study area consists of the entirety of the Big Boggy Creek watershed, outlined in red. The blue stars mark the location of sensor stations at Upper Boggy (UB), Lower Boggy (LB), and Chinquapin Road (CR).

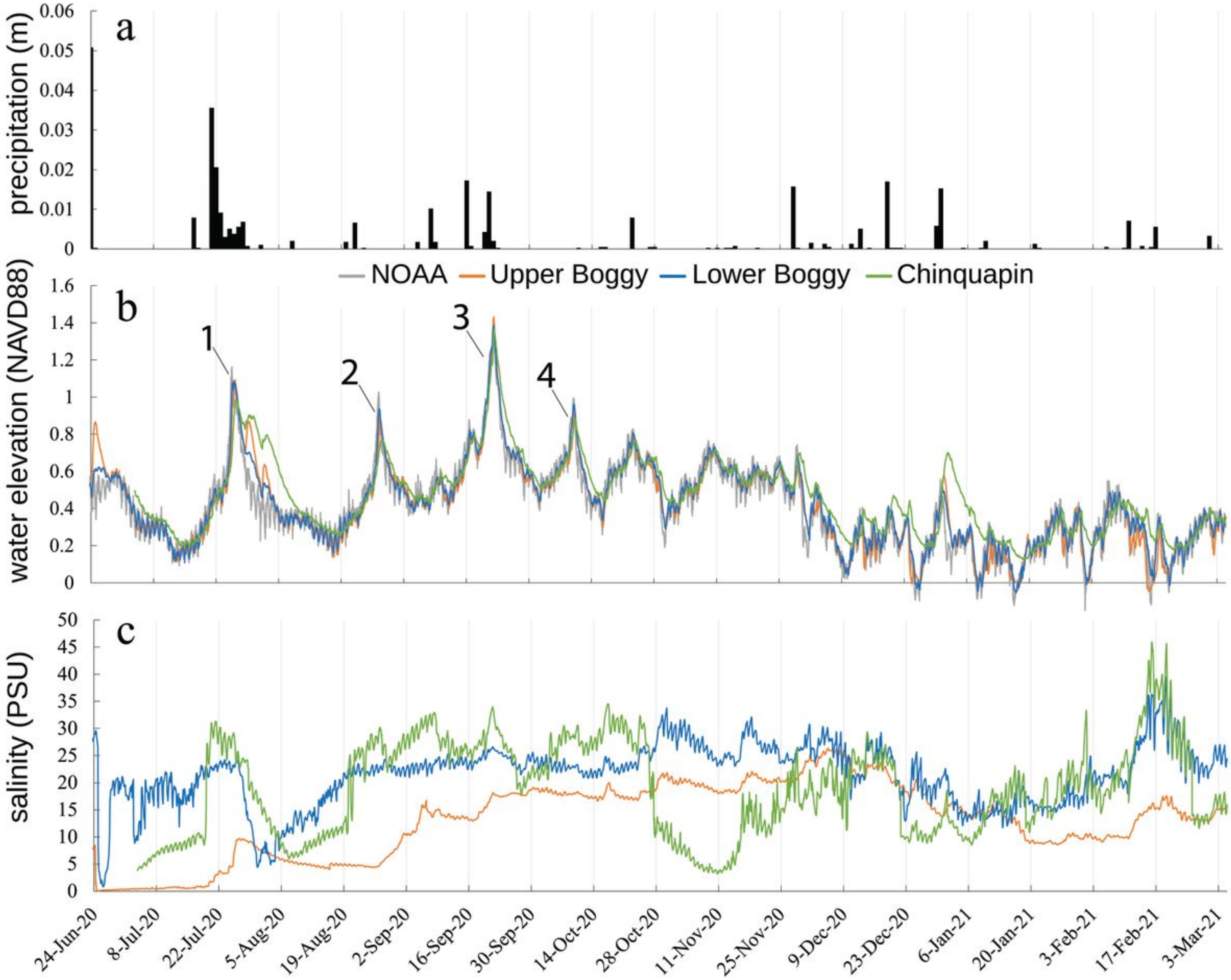

Figure 2

Precipitation (a), water elevation (b), and salinity (c) as obtained from the LCRA rain gauge (a) and the deployed CTDs (b, c). Water elevation is in NAVD88 meters. Salinity is in Practical Salinity Units (PSU), which is similar to a parts per thousand (ppt) measurement. Named tropical cyclones that occurred during the study period and the resulting peak water elevation are indicated as (1) Hurricane Hanna, (2) Hurricane Laura, (3) Tropical Storm Beta, and (4) Tropical Storm Delta.

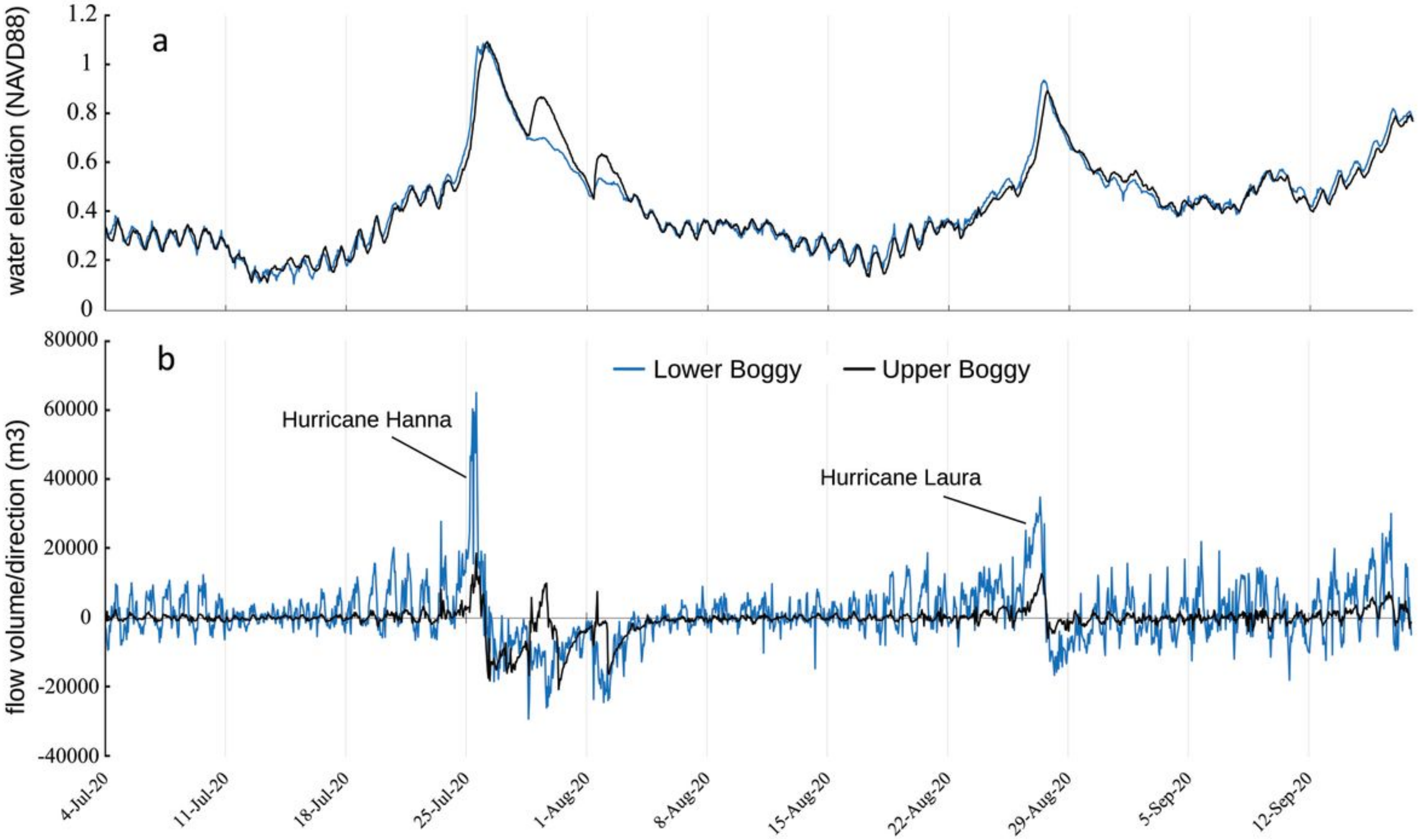

Figure 3

Water elevation (a) and flow volume/direction (b) measured by ADCPs at Upper and Lower Boggy stations. Positive values indicate upstream flows, negative values indicate downstream flows. Hurricane Hanna and Hurricane Laura events were captured by the ADCPs and are indicated at their respective peak flow volumes.

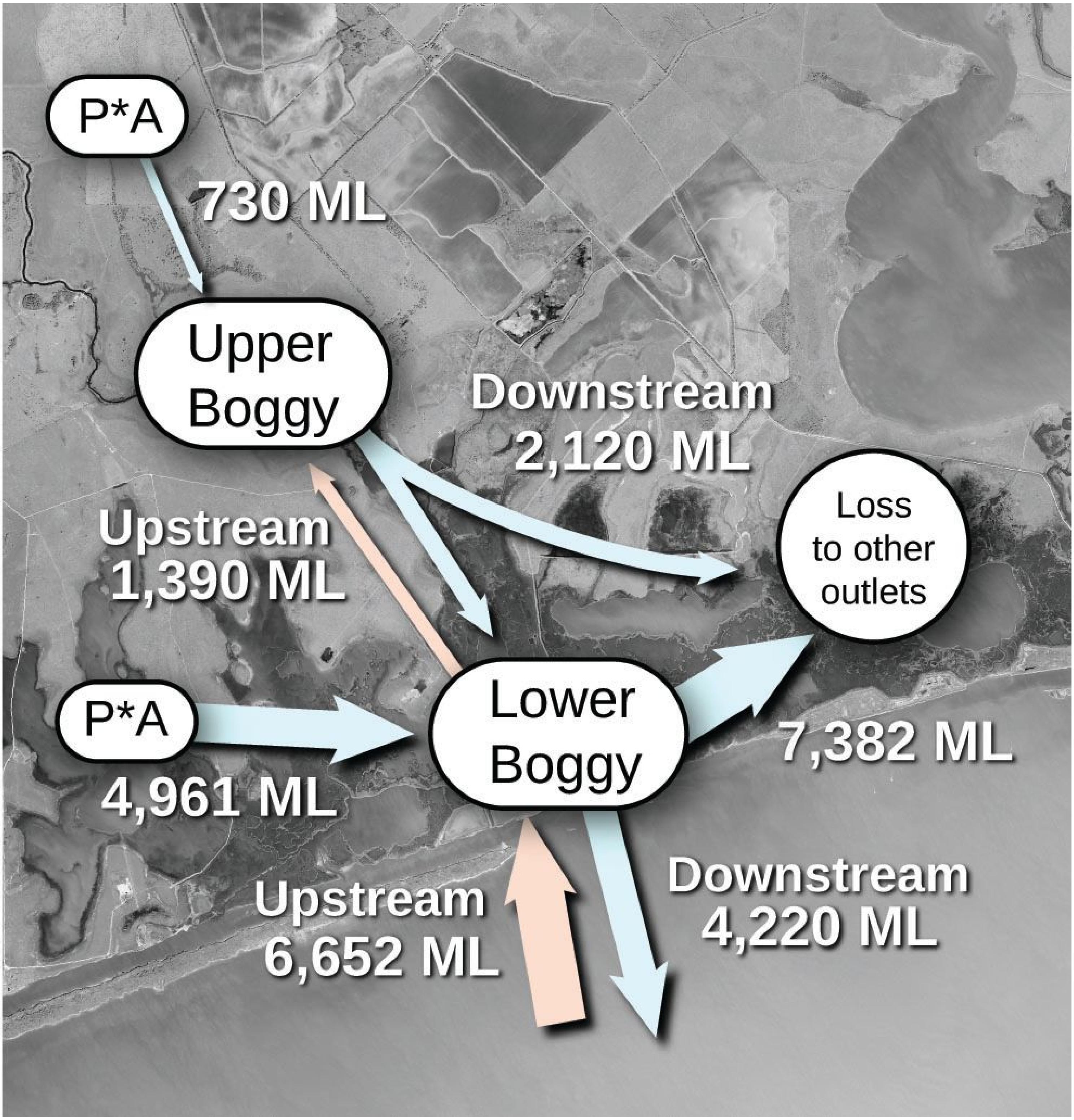

Figure 4

A visualization of the water budget for Big Boggy Creek from July 2020 to September 2020. Units are in megaliters (ML). Measured precipitation (P) multiplied by the effective watershed area (A) equals the precipitation volume captured by the sensors.

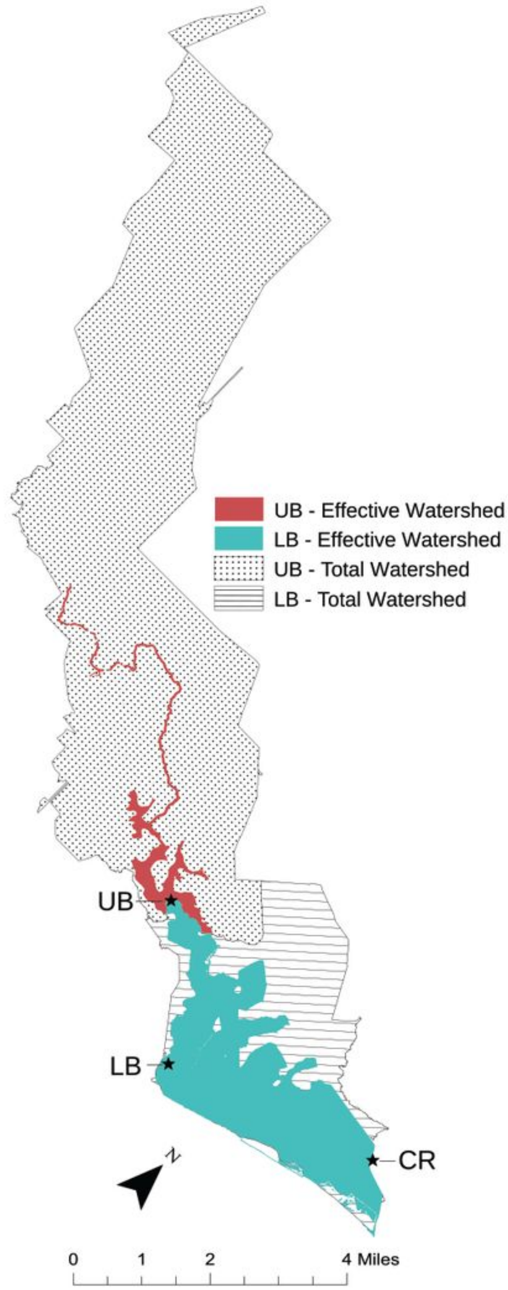

Figure 5

The Big Boggy Creek watershed delineated into four sections: the Upper Boggy (UB) effective watershed, the Lower Boggy (LB) effective watershed, the UB total watershed, and the LB total watershed. The black stars depict the sensor locations for Upper Boggy (UB), Lower Boggy (LB), and Chinquapin Road (CR).

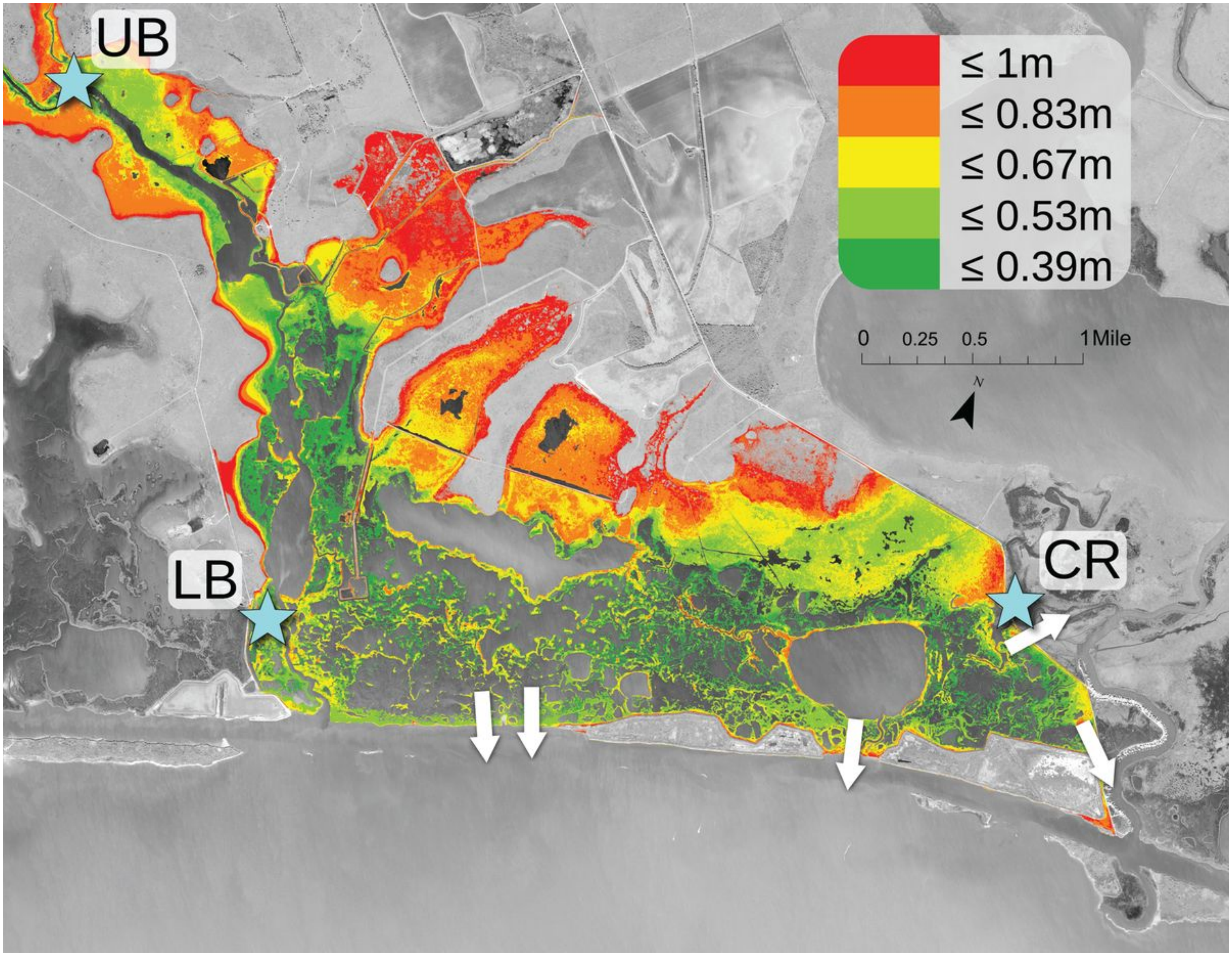

Figure 6

Alternate outlets for flowing water (white arrows) and water elevations needed to flood portions of the watershed (NAVD88 meters). Upper Boggy (UB), Lower Boggy (LB), and Chinquapin Road (CR) sites are depicted as blue stars.

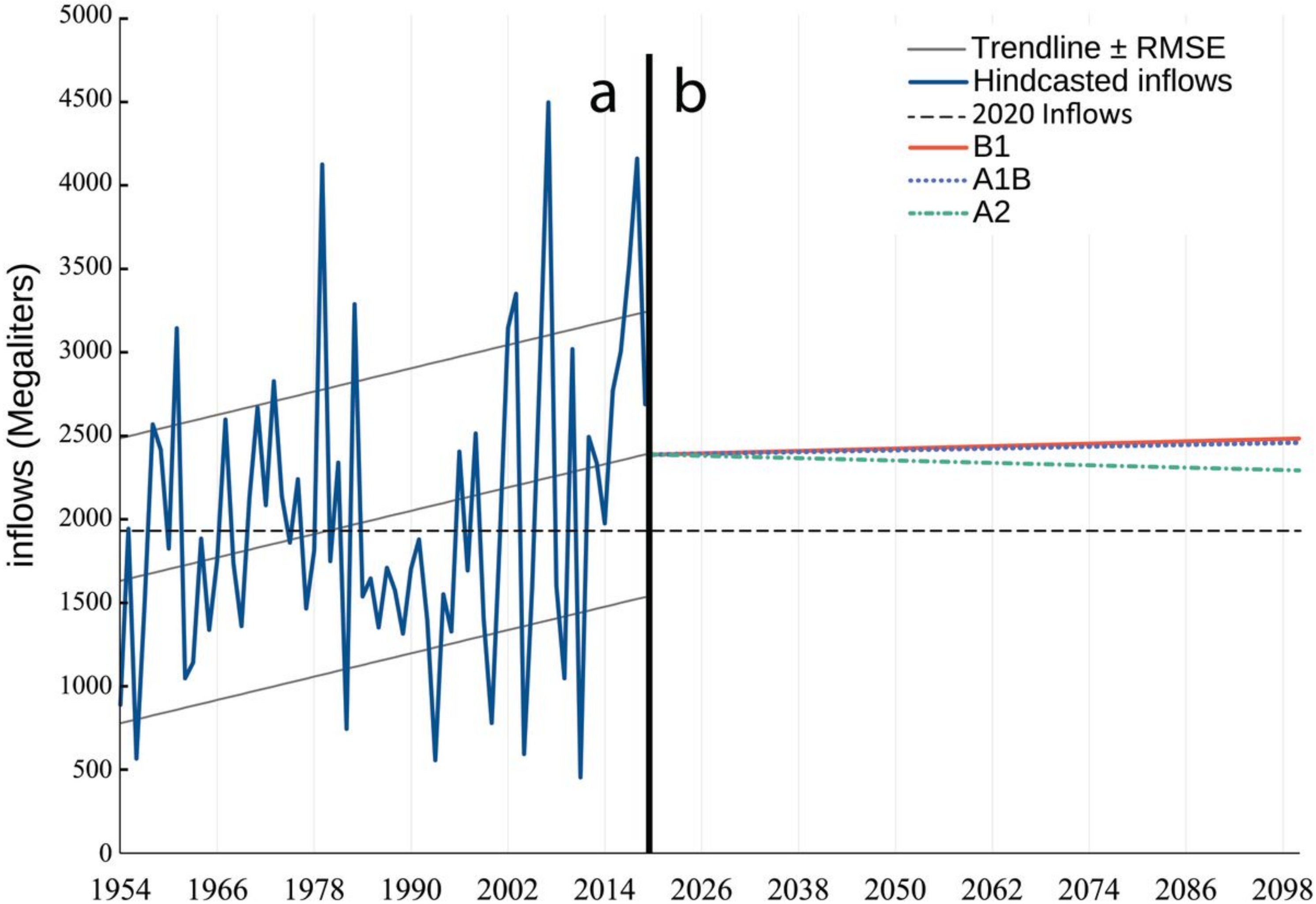

Figure 7

Hindcasted (part (a) on the left; 1954 – 2019) and forecasted (part (b) on the right; 2021 – 2100) inflows at Upper and Lower Boggy combined. The inflow rates that we observed in the field in 2020 are depicted (dashed line) for comparison. For each year, only three months were used to match the 2020 study period (July, August, and September).